Number of Text Pages: 34

Number of Tables: 1

Number of Figures: 2

Title: Metabolic alterations proposed by proteome in rice roots grown under low P and high Al concentration under low pH.

Running Title: Proteomic alterations in rice roots grown under low P and high Al

Authors: Takuya Fukuda[12], Akira Saito[1], Jun Wasaki[3], Takuro Shinano[3] and Mitsuru Osaki[1]

Affiliation: [1] Graduate School of Agriculture, Hokkaido University

[2] In present, Photobiology and Photosynthesis Research Unit, National Institute of Agrobiological Sciences

[3] Creative Research Initiative 'Sousei' (CRIS), Hokkaido University

Address: [1] N9W9, Kita-ku, Sapporo 060-8589, Japan

[2] In present, 2-1-2 Kannondai, Tsukuba, Ibaraki 305-8602, Japan

[3] N21W10, Kita-ku, Sapporo 001-0021, Japan

Corresponding Author: Jun Wasaki

E-mail: junw@chem.agr.hokudai.ac.jp

Tel & Fax: +81-11-706-9286

Abstract

Growth inhibition caused by acid soils, especially due to P deficiency and Al stress, is a serious problem for crop production. To comprehend the adaptation mechanisms of rice plants to P deficiency and Al stress conditions, a proteomic analysis of rice roots in hydroponic cultivation was demonstrated. 464 detectable proteins spots were separated by 2D-PAGE. 56 of 94 spots selected at random were identified by peptide mass fingerprinting. In general, the proteomic alterations under P deficiency and Al stress conditions were similar trend, indicating that a common metabolic system is responsive to both P deficiency and Al stress. An increase in nucleotide monomer synthesis was indicated from the related proteomic alterations, which mediate the reversible reactions of the triose phosphate/pentose phosphate pool, and the oxidative reactions of the pentose phosphate pathway under both stress conditions. Carbon flow to the TCA cycle and N assimilation were altered in proteomic level. The changes could be contributed to the complementation of TCA components from suppression of photosynthates partitioning from leaves, and partly contribute to organic acid secretion. Induction of S-adenosylmethionine (SAM) synthetase is a significant and unique response to Al stress, suggesting that SAM is related to ethylene-mediated inhibition of root growth and/ or the alteration of cell wall structures and polymers in roots.

Abbreviations: ACC, 1-aminocyclopropane-1-carboxylic acid; ADK, adenosine kinase; 2D-PAGE, 2 dimensional polyacrylamide gel electrophoresis; DTT, dithiothreitol; PEPC, phospho*enol*pyruvate carboxylase; Pi, inorganic phosphate; PMF, peptide mass fingerprinting; SAH, S-adenosyl-L-homocysteine; SAM, S-adenosylmethionine.

Key Words; Proteomics, Low pH, Low Phosphorus, Aluminum stress, Rice

Introduction

Growth inhibition caused by acidic soils, especially due to P deficiency and Al stress, is a serious problem for the production of many of the world's important crops. Acid soils are distributed worldwide, and 30 – 40% of the world's soils are below pH 5.5 [1]. Marschner [2] has summarized the major constraints of acid soil on plant growth as H^+, Al and Mn toxicity, Mg, Ca, K, P and Mo deficiency, and inhibition of root growth and water uptake. Of these, P deficiency and Al stress are the most serious problems.

Plants employ several strategies to obtain P efficiently when they grow under low P conditions. Roots grown under P-deficient conditions secrete acid phosphatase (APase) to release inorganic phosphate (Pi) from organic compounds, and organic acids to release Pi from insoluble inorganic phosphate compounds [3,4]. Several genes related to low P adaptation have been isolated. Secreted APase, designated as *LASAP2*, has been isolated from white lupin [5]. It was also reported that gene expression of a high affinity Pi transporter increased in roots of P-deficient plants [6-9]. To increase root surface area, the diameter of main roots is decreased and the number of root hairs is increased [10]. Proteaceae and lupin plants develop bottle-brush like clustered roots, known as 'cluster roots' or 'proteoid roots', under P deficient conditions [3,11-13]. The function of these roots is not only to increase root surface area, but also to stimulate vigorous inorganic phosphate liberation from unavailable forms by secretion of

APase and organic acids, and overexpression of Pi transporters [7,14,15].

Plants have a number of mechanisms to maximize the efficient use of absorbed P. The bypass pathway, which substitutes Pi- and adenylate-requiring enzymes with pyrophosphate- and NADP-dependent enzymes, conserves Pi rather than producing energy [16,17]. Production of ribonucleases also increases under P deficiency to mobilize Pi from internal RNA pools [18-21]. Phospho*enol*pyruvate carboxylase (PEPC) not only serves as the alternative pathway supplying carbon skeleton to the TCA cycle but also for Pi recycling via the PEP-consuming and glycolate pathways [22].

Al is the most common among metallic elements in the soil. It is sparingly soluble in neutral pH and is thus innocuous. At low pH, however, the soluble Al ions are toxic. The distinctive toxicity is manifest as the inhibition of root growth, Al accumulation on the root surface, induction of callose synthesis and lignin accumulation. Lipid peroxidation in the plasma membrane and inhibition of Ca^{+} channel transport, altered transcription of mRNA, and inhibition of DNA synthesis are also considered as expressions of solubilized Al toxicity.

Al tolerance is apparently due to both apoplastic and symplastic mechanisms. Selective permeability of the plasma membrane, induction of a pH barrier in the rhizosphere, release of chelating ligands and secretion of Pi and Al have been proposed as apoplasmic mechanisms [23]. Much of the research on Al tolerance, however, has centered on organic acid

secretion. Plant roots grown under Al stress secrete organic acids and moderate the toxicity of Al ions by chelation [24]. A viscous mucilage, consisting mainly of polysaccharides, is secreted from roots and may act as a barrier to Al toxicity [25,26]. Moderation by organic acids, proteins, and other ligands, accumulation of Al in vacuoles, and activation of Al-tolerant enzymes have been suggested as symplasmic tolerance mechanisms [27].

Adaptation mechanisms to P deficiency and Al stress have been proposed by transcriptomic analyses [28-34]. Wu *et al*. [33] and Hammond *et al*. [28] reported that the expression of various genes in *Arabidopsis*, such as those involved in the bypass pathways of C metabolism and signal transduction, changes when plants are grown under low-P conditions. Wang *et al*. [31] developed microarrays containing mineral nutrition-related cDNAs to analyze the transcriptomic changes caused by P, K and Fe deficiency, suggesting that deficiency of these three essential elements caused cross-talk during gene regulation. Wasaki *et al*. [32] reported some low P adaptation strategies, such as the enhancement of C skeleton supply required for organic acid exudation and alteration of lipid metabolism.

Transcriptomic analysis provides a lot of information, but knowing which genes are transcribed, and when, is not enough to understand the full extent of metabolic changes because of post-transcription and post-translation modifications. In fact, Anderson and Seihamer [35] reported that the correlation factor between the number of transcripts and translated protein was

below 0.5. Only a few reports have addressed the expression of root proteins as a whole [36-38]. In the current study, proteomic analysis was applied to comprehend the metabolic network of alterations in rice roots caused by low P and high Al under low pH hydroponic conditions. Total protein from roots was separated by 2D-PAGE and profiled. The spots were identified by Edman sequencing and peptide mass fingerprinting (PMF).

Materials and Methods

Plant Material

Rice (*Oryza sativa* L. cv Michikogane) seeds were surface sterilized in 1% $(HClO)_2Na$ for 10 min and then incubated in tap water overnight. All cultures were hydroponically conducted at greenhouse. The seeds were transferred into a 56 L container and germinated on a net floated on tap water for 3 weeks. Seedlings were transferred to nutrient solution in a 56 L container containing 1.07 mM NH_4NO_3, 0.03 mM $NaH_2PO_4 \cdot 2H_2O$, 0.39 mM K_2SO_4, 0.39 mM KCl, 1.25 mM $CaCl_2 \cdot 2H_2O$, 0.82 mM $MgSO_4 \cdot 7H_2O$, 35.8 µM $FeSO_4 \cdot 7H_2O$, 9.1 µM $MnSO_4 \cdot 4H_2O$, 46.3 µM $ZnSO_4 \cdot 7H_2O$, 0.16 µM $CuSO_4 \cdot 5H_2O$, and 0.05 µM $(NH_4)_6Mo_7O_{24} \cdot 4H_2O$. The pH of the solution was adjusted to 5.0 every day. After 2 weeks, seedlings were transplanted to low pH (4.5) solution and cultivated for 7 days to habituate them to low pH conditions, and then transferred to the control standard nutrient solution, or to the experimental stress treatment solutions containing either no phosphorus (–P) or Aluminum (+Al) (3 mM $Al_2(SO_4)_3 \cdot 18H_2O$ in the standard solution). The pH of each solution was adjusted to 3.5 daily. The Pi concentration of the control and +Al solutions was adjusted daily to compensate for plant assimilation.

The plants were collected 0, 1, 3 and 5 d at daytime and 0.5 d at nighttime with four

replications of four plants per replication after transfer to the treatment and control solutions. Rice plants grown in control and –P solutions were also collected 10 d after transplanting. Roots were separated, frozen in liquid nitrogen and stored at -80 ˚C until protein extraction.

Extraction of Protein

Whole roots were homogenized using pestle and mortar containing liquid nitrogen. One hundred mg of polyvinylpolypyrrolidone and 2 mL of extraction buffer (20 mM Tris-HCl, 400mM NaCl, pH7.5) were added to a 1 g sample of homogenized root tissue. The suspension was centrifuged at 4˚C and 11,833 x *g* for 10 min and the supernatant was re-centrifuged for 5 min. An equal amount of TCA/acetone solution (20% (w/v) trichloroloacetic acid, 0.14% (w/v) dithiothreitol [DTT] in acetone) was added to the supernatant and incubated at -20˚C for 30 min. The suspension was sonicated two times for 10 min on crushed-ice water, and centrifuged at 4˚C for 15 min. The supernatant was discarded and 1.5 mL of acetone containing 0.07% DTT was added to the pellet for sonication on crushed-ice water until the pellet was completely resuspended. The precipitated protein was washed in acetone containing 0.07% DTT, pelleted at 4˚C and 11,833 x *g* for 15 min, dried in a vacuum desiccator and dissolved in 100 µL of lysis buffer (7 M Urea, 2 M thiourea, 4% CHAPS, 65 mM DTT) by sonication for 15 min on crushed-ice water. Protein concentration was measured according to Bradford [39].

2D-PAGE

2D-PAGE was performed with 4 replications of each treatment as below. A tube gel containing 4% acrylamide, 8 M Urea, 2% Triton X-100 and 2% ampholine (1% each Bio-Lyte 5/8 and Bio-Lyte 3/10; Bio-Rad Laboratories, Hercules, CA, USA) was used to separate the crude proteins in a 300 µg aliquot containing ampholine at the same concentration as the tube gel by pI. The cathode solution consisted of 20 mM NaOH and the anode solution was 10 mM H_3PO_4. The protein was electrophoresed using equipment for tube gel electrophoresis (NA-1313B; Nippon Eido, Tokyo, Japan) at room temperature for 0.5 h at 200 V constant voltage, for 16 h at 400 V constant voltage and then for 60 min at 600 V constant voltage.

The tube gel was equilibrated twice in 625 mM Tris-HCl (pH6.8) containing 4% SDS, 5% 2-mercaptoethanol, 0.0025% BPB for 15 min, transferred in the dark to 5 mL of carbamoyl methylation buffer containing 30 mM Tris-HCl at pH 6.8, 2.5% w/v SDS, 300 mM iodoacetamide and 0.003% w/v bromophenol blue for 15min and applied to the top of the SDS-PAGE gel. The tube gel was fixed in place by overlaying melted 0.5% agarose containing 250 mM Tris-HCl (pH 6.8) and 0.1% SDS. SDS-PAGE was performed using a Protean IIxi cell (Bio-Rad Laboratories) for 40 min at 120 V constant voltage, then for another 5 h at 190 V constant voltage using concentration (5%, 125mM Tris-HCl, 0.1% SDS, pH6.8) and separation

gels (10% acrylamide, 375 mM Tris-HCl, 0.1% SDS, pH8.8) according to Laemmli [40]. The running buffer was 25 mM Tris, 192 mM Glycine and 0.1% SDS.

Separated protein was stained with Coomassie Brilliant Blue. The stained gel was scanned (EPSON ES-2200, Seiko Epson, Nagano, Japan) and analyzed using PDQuest software (Bio-Rad Laboratories). The strength of detected spots was determined and averaged for 4 electrophoresed digital images. Background intensity was used for each missing spot to analyze the modifications of protein expression during treatments. To accurately compare spot quantities between gels, some variation in spot intensity was globally normalized by lowess (locally weighted linear regression) fitting, as well as the same method of microarray data normalization. The normalization is based on robust local regression, implemented in the statistical software package R [41] to perform the linear fits with lowess (locally weighted linear regression) scatter plot smoother [42]. The effect on each treatment was evaluated as log ratio (treatment / control) for each data point. After normalization, hierarchical cluster analysis was performed to identify relatively homogeneous groups of protein expression using average linkage between groups algorithm and cosine coefficient in software packages SPSS 13.0 software (SPSS Inc., USA). The significant differences of the signal intensities between control and treatment were analyzed for all time points by ANOVA.

Identification of Separated Proteins

Stained gels were transferred to Sequi-blot™ PVDF Membranes (Bio-Rad Laboratories) for Edman sequencing of N-terminal amino acids [43]. Only distinct spots were applied to an amino acid sequencer (Procise™ 491-HS Protein Sequencing Systems; Applied Biosystems, Foster City, CA, USA).

Randomly selected spots were cut from the gel and transferred to a multiwell plate. The spots were digested with trypsin (Promega, Madison, MI, USA) for peptide mass fingerprinting using time of flight mass spectrometry (TOF-MS) (Voyager DE-STR/15000; Applied Biosystems) according to Toda and Kimura [44] (summarized in http://proteome.tmig.or.jp/2D/2DE_method.shtml). AcTH18~39 and Angiotensin I (Sigma-Aldrich, St. Louis, MO, USA) were used as standards. A database search of peptide mass fingerprints was performed using Mascot software [45].

Results

Overview of root growth response and identified spots

Root growth was slightly enhanced a few days after –P treatment, whereas inhibited by Al stress (Table 1). A master image, which was produced as a composite of all analyzed gel images, is shown in Figure 1. 464 spots were detected with 2D-PAGE. Peptide mass fingerprinting (PMF) of 94 spots selected at random resulted in the identification of 56 spots. Edman sequencing successful for 3 spots (ssp5310, 6304 and 3411), giving N-terminal amino acid sequences corresponding to PMF, thus supporting the reliability of PMF identification. The list of identified proteins and the relative amounts of each identified spot are in the Table 2.

Nearly half of the 56 identified spots were involved in C metabolism. Nitrogen-related metabolism (4 spots), nucleotide-related (4 spots) and oxidation/reduction--related proteins (8 spots) were also identified (Table 2). Some relatively constitutive proteins, such as 2 actin isoforms, are also listed (Table 2).

Five sets of 2 or 3 spots had same accession number, though detected in other places (Figure 1 and Table 2; ssp4801 and 4804, transketolase; ssp5307, 5310 and 6304, glyceraldehyde 3-phosphate dehydrogenase; ssp7301 and 7305, cytosolic glyceraldehyde 3-phosphate dehydrogenase; ssp2701 and 2711, trypanothione-dependent peroxidase; ssp3105

and 4101, L-ascorbate peroxidase). This suggested that modifications of the same protein caused the protein spots to shift, possibly due to expression of alternate alleles or post-translational modifications. Among the shifted proteins, 4 sets had a similar expression pattern (Table 2). In the case of glyceraldehyde 3-phosphate dehydrogenase, an isoform detected as ssp5307 was regulated by both low P and Al stress.

A large number of proteins were up- or down-regulated during the treatment. When an increase of 100% was used as the criterion for defining up-regulation (i.e. 2-fold increase), 15 proteins were up-regulated among the identified spots. 29 proteins were increased at the 50% increase threshold (i.e. 1.5-fold increase). When the criteria were a reduction to half of the expression in the controls (i.e. 2-fold reduction) 14 spots were down-regulated. 24 spots had a decrease in intensity to two-thirds of the control (i.e. 1.5-fold reduction) by –P treatment at any point in time (Table 2). 14 and 24 spots were up-regulated at the 2- and 1.5-fold levels and 11 and 17 spots were down-regulated by the 2.0 and 1.5 fold levels by Al treatment (Table 2), respectively. These alteration data could be possible to assess the reliability by the mode of standard errors for all datasets of each treatment, which is 0.57 for $\log_2$(-P/+P) data sets and 0.57 for $\log_2$(+Al/-Al).

Proteomic alterations related to carbon metabolism

Fructokinase I (ssp2311) was transiently up-regulated at 0.5 d by Al stress. Fructosebisphosphate aldolase (ssp6410) was at a low level in both treatments with a maximum decrease at 5 d in the +Al treatment. An isoform of glyceraldehyde 3-phosphate dehydrogenase (ssp5307) was expressed at a lower level in the –P treatment than in the control plants at each time period except at 1 d.

In the triose phosphate/pentose phosphate pool pathways, transketolase (ssp4801 and 4804) was up-regulated at 0.5 d in both treatments. UDP-glucose dehydrogenase (ssp4608) had its maximum decrease at 3 d in both treatments. UDP-glucose pyrophosphorylase (ssp4503) peaked at 3 d in both treatments. 6-phosphogluconate dehydrogenase (ssp5511) oscillated during the Al treatment.

Most but not all TCA cycle-related enzyme expression was relatively constant over time. Cytoplasmic malate dehydrogenase (ssp4311), mitochondrial malate dehydrogenase (ssp5306, except at 1 d in –P treatment), dihydrolipoamide dehydrogenase (ssp6603), citrate synthase (ssp6501) and NADP-specific isocitrate dehydrogenase (ssp5416) did not change significantly. Aconitate hydratase (ssp4911) was strongly up-regulated at 1 d in both treatments and at 10 d in the –P treatment. Malic enzyme (ssp4711) was down-regulated at 3 d in the +Al treatment and up-regulated at 10 d in the –P treatment. Succinate dehydrogenase (ssp5708) was down-regulated at 5 d under Al stress.

Comparison between –P and Al stress

All 464 detected spots were subjected to hierarchical cluster analysis to identify relatively homogeneous groups of protein expression. As the results, the modifications of root protein expression under P deficiency and Al stress were similar (Supplemental Figure 1). In general, the proteomic alterations were similar trend in both treatments although the counter ions such as Na^{+} and SO_4^{-2}, which are always essential in hydroponics, might affect the metabolic responses. It is likely that this is due to the similarity in adaptation strategies, such as the secretion of organic acids. Malic enzyme (ssp4711), dihydrolipoamide dehydrogenase (ssp6603), thioredoxin reductase (ssp5309), aconitate hydratase (ssp4911), mitochondrial malate dehydrogenase (ssp5306) and two S-adenosylmethionine (SAM) synthetases (ssp4416 and 5402) responded differently to –P and +Al treatments, with the largest difference in the response of the two SAM synthetases (ssp4416 and 5402).

Discussion

It has been reported that P deficiency generally influences carbon metabolism end products such as secretion of organic acids from roots, starch accumulation in shoots, and bypass pathways for recycling internal Pi. Al stress also affects organic acid exudation, alteration of cell wall structures, and prevention of gene expression by binding Al to nucleotides. However, responses to P deficiency and Al stress on the metabolic network are unclear. The proteomic analyses in this study indicate that P deficiency and/or Al stress are implicated in adjustments to nucleotide synthesis and related carbon pathways the glycolytic pathway, and cell wall structure.

Nucleotide synthesis and related carbon pathways affected by P deficiency and Al stress

Proteomic responses to P deficiency and Al stress on carbon metabolism are summarized in Figure 2. Interpreting from the response of fructokinase I (ssp2311), fructosebisphosphate aldolase (ssp6410) and glyceraldehyde 3-phosphate dehydrogenase (ssp5307), fructose 6-phosphate would be transiently synthesized at first, whereas fructose 6-phosphate and glyceraldehyde 3-phosphate could be supplied to the triose phosphate/pentose pool with the decline of fructose-bisphosphate aldolase and glyceraldehyde 3-phosphate

dehydrogenase. Up-regulation of transketolase (ssp4801 and 4804) could provide ribose 5-phosphate reversibly, since ribose 5-phosphate is well known as a substrate of nucleic acid synthesis. The increased activity of this enzyme could be concerned with meeting the demand of RNA synthesis. The up-regulation of cytidine deaminase (ssp3311) supports this speculation because it is involved in uridine and deoxyuridine synthesis. In earlier transcriptomic studies, a dynamic change of transcripts was found under low P stress conditions [28,30-33] and Al stress conditions [34].

DNA damage is a well known phenomenon of Al toxicity [46-48]. Matsumoto [49] proposed that DNA-Al complex formation and repression of transcription by Al could be a major cause of reduced root growth. The increase in nucleotide monomer concentration is a reasonable adaptation phenomenon under these stress conditions.

The expression of 6-phosphogluconate dehydrogenase (ssp5511) oscillated during +Al treatment. This enzyme synthesizes ribulose 5-phosphate with the formation of NADPH. A decrease in the enzyme at 1 d coincides with an increase of transketolase. Moreover, the increase in 6-phosphogluconate dehydrogenase over 3 d also coincides with changes in UDP-glucose dehydrogenase and UDP-glucose pyrophosphorylase levels. Adaptation to high Al concentrations may not be limited to the reversible reactions of the triose phosphate/pentose phosphate pool, as the oxidative reactions of the pentose phosphate pathway also could be

regulated during Al treatment.

Effect of –P for 10 d on glycolysis

Ten days after removal of P, many glycolysis-related proteins were up-regulated and a glutamate synthase was down-regulated (Table 2). This result corresponded with the results of transcriptomic analyses in rice roots by Wasaki *et al*. [32] suggesting that several genes related to glycolysis are up-regulated and that ammonium assimilation-related genes are down-regulated when held under P-deficiency treatment for 9 d. Not only in monocot plants, also in dicotyledonous Arabidopsis roots and leaves, the genes involved in N assimilation were down-regulated after 24 h of Pi starvation [33]. Uhde-Stone *et al*. [30] also reported that some glycolytic pathway related genes were induced in P-deficient white lupin proteoid roots. Wasaki *et al*. [32] concluded that the stimulation of glycolysis contributes to the acceleration of carbon skeleton supply for organic acid synthesis. Proteomic data also supports this conclusion. The down-regulation of ammonium assimilation-related genes and proteins supports this speculation, because organic acid synthesis consumes carbon skeleton molecules as a source of amino acids.

The supply of carbon skeleton molecules by the acceleration of glycolysis seems appropriate for organic acid secretion as proposed in a previous paper [32], because it has been

reported that rice roots secrete citrate or oxalate [50,51]. However, the amount of oxalate secreted from rice roots was at a markedly lower level than the amount of citrate or malate secreted from other plants that have a significant tolerance for low P or Al stress. Begum *et al*. [49] showed that the total organic acid concentration in rice roots grown under reduced P was similar level to conditions with sufficient P. Rice plants are able to grow well even under internal low P content conditions. Thus, the main tolerance strategies to low P conditions would be the efficient utilization of internal P. In fact, it has already been shown that the activities of internal phosphatase and ribonuclease increase under low P conditions [52]. Furthermore, Nanamori *et al*. [52] concluded that strategies for low P tolerance in rice involves (1) decreased carbon flow to amino acids and organic acids, and decreased N concentration; and (2) improved partitioning of photosynthates to sucrose, combined with restricted sugar catabolism. We conclude, then, that the carbon flow to the TCA cycle and repression of N assimilation indicated in this study (Table 2) and in previous transcriptomic data [32] contribute to the complementation of TCA components from suppression of photosynthates partitioning from leaves, and contribute partly to organic acid exudation.

Induction of SAM synthetase by Al stress

Massot *et al*. [53] reported that a rapid increase of ethylene evolution precedes

aluminum ion-induced inhibition of root growth in bean. Although SAM is the precursor of ethylene, it is known that the key enzyme of ethylene synthesis is 1-aminocyclopropane-1-carboxylic acid (ACC) synthase. Since ACC synthase was not identified in this study, further research is required to determine whether the up-regulation of SAM synthetase is involved in ethylene-mediated inhibition of root growth.

Stimulation of SAM synthesis could be involved in the alteration of cell wall and polymer structures in roots. Using an adenosine kinase (ADK) mutant, Moffatt *et al*. [54] showed that the hydrolysis of S-adenosyl-L-homo-cysteine (SAH) produced from SAM-dependent methylation reactions is a key source of adenosine in plants. ADK activity and the level of methylesterified pectin in seed mucilage were correlated directly in their experiments. Root mucilage exudation is considered to be an aluminum toxicity prevention strategy [55,56], since the modification of mucilage seems to be a reasonable response under Al stress conditions. Shen *et al*. [57] reported the decrease of lignin, which is known as a metabolic sink of SAM, in a SAM synthetase-3 gene mutant in *Arabidopsis*. These observations are corroborated by the maximum down-regulation of UDP-glucose dehydrogenase (ssp4608) at 3 days in +Al treatments in the present study (Table 2). UDP-glucose dehydrogenase synthesizes UDP-glucuronate, which is a precursor of hemicellulose and pectin. In addition, a recent transcriptomic experiment revealed that cellulose synthase was also up-regulated in Al tolerant

wheat cultivar, as reported by a review article [34]. The structure of cell wall polymers in roots may be important under Al stress conditions, though further experiments are necessary to understand their function.

Conclusion

In present study, 56 protein spots extracted from rice roots were identified. Many of them were regulated by P deficiency and Al stress, which are limiting factors on the growth of plants in acid soils. The effects of P deficiency and Al stress on metabolic adaptations are likely to be reflected in the expression of root proteins. A comparison of the proteins present in roots grown under aluminum stress, phosphorus deficiency and control conditions suggests that; 1) in general, modifications of root protein expression under P deficiency and Al stress were similar, 2) nucleotide synthesis was stimulated by P deficiency and Al stress, 3) carbon flow to the TCA cycle was maintained by stimulation of glycolysis by P deficiency for 10 d, and 4) Al stress caused changes in some cell wall structures. Some of these protein expression changes have not yet been demonstrated by transcriptomic analyses. Because proteins can now be quickly mapped on 2-DE gel and identified, the proteomic analyses can generate an accurate and rapid catalog of enzymes and structural proteins under any set of growth conditions. Proteomic analysis is thus a useful tool for understanding the physiological alterations of plant roots under

abiotic stress.

Acknowledgments

This research was partly supported by a grant from the Ministry of Agriculture, Forestry and Fisheries of Japan (Rice Genome Project MA-2111 & PR-1217) and Grant-in-Aid from Ministry of Education, Culture, Sports, Science and Technology (16208008).

References

[1] H.R. von Uexküll, E. Mutert, Global extent, development and economic impact of acid soils, Plant Soil 171 (1995) 11-15

[2] Marschner H. Mineral Nutrition in Plants. 2nd edition, Academic Press. San Diego, CA, 1995.

[3] W.K. Gardner, D.A. Barber, D.G. Parbey, The acquisition of phosphorus by *Lupinus albus* L. III. The probable mechanism by which phosphorus movement in the soil/root interface is enhanced, Plant Soil 70 (1983) 107-124.

[4] T. Tadano, H. Sakai, Secretion of acid phosphatase by the roots of several crop species under phosphorus-deficient conditions, Soil Sci. Plant Nutr. 37 (1991) 129-140.

[5] J. Wasaki, M. Omura, M. Ando, H. Dateki, T. Shinano, M. Osaki, H. Ito, H. Matsui, T. Tadano, Molecular cloning and root specific expression of secretory acid phosphatase from phosphate deficient lupin (*Lupinus albus* L.). Soil Sci. Plant Nutr. 46 (2000) 427-437.

[6] M. Kai, K. Takazumi, H. Adachi, J. Wasaki, T. Shinano, M. Osaki, Cloning and characterization of four phosphate transporter cDNAs in tobacco, Plant Sci. 163 (2002) 837-846.

[7] J. Liu, C. Uhde-Stone, A. Li, C. Vance, D. Allan, A phosphate transporter with enhanced expression in proteoid roots of white lupin (*Lupinus albus* L.), Plant Soil 237 (2001) 257-266.

[8] U.S. Mucchal, J.M. Pardo, K.G. Raghothama, Phosphate transporters from the higher plant *Arabidopsis thaliana*, Proc. Natl. Acad. Sci. USA 93 (1996) 10519-10523.

[9] U.S. Mucchal, K.G. Raghothama, Transcriptional regulation of plant phosphate transporters, Proc. Natl. Acad. Sci. USA 96 (1999) 5868-5872.

[10] J. Lynch, Root architecture and plant productivity, Plant Physiol. 109 (1995) 7-13.

[11] M.W. Shane, M. De Vos, S. De Roock, H. Lambers, Cluster root growth and citrate exudation in *Lupinus albus* L. (white lupin): Separating the influences of root and shoot phosphorus. Plant Cell Environ. 26 (2003) 265–273.

[12] K.R. Skene, Cluster roots: some ecological considerations, J. Ecol. 86 (1998) 1060-1064.

[13] M. Watt, J.R. Evans, Proteoid roots. Physiology and development, Plant Physiol. 121 (1999) 317-323.

[14] J. Wasaki, T. Yamamura, T. Shinano, M. Osaki, Secreted acid phosphatase is expressed in cluster roots of lupin in response to phosphorus deficiency, Plant Soil 248 (2003) 129-136.

[15] G. Neumann, E. Martinoia, Cluster roots – an underground adaptation for survival in extreme environments, Trends Plant Sci. 7 (2002) 162-167.

[16] S.M.G. Duff, G.B.G. Moorhead, D.D. Lefevbre, W.C. Plaxton, Phosphate starvation inducible bypasses of adenylate and phosphate dependent glycolytic enzymes in *Brassica nigra* suspension cells, Plant Physiol. 90 (1989) 1275-1278.

[17] S.M.G. Duff, W.C. Plaxton, D.D. Lefebvre, Phosphate-starvation response in plant cells: De novo synthesis and degradation of acid phosphatases, Proc. Natl. Acad. Sci. USA 88, (1991) 9538-9542.

[18] D. Bosse, M. Köck, Influence of phosphate starvation on phosphohydrolases during development of tomato seedlings, Plant Cell Environ. 21 (1998) 325-332.

[19] P.J. Green, The ribonucleases of higher plants, Ann. Rev. Plant Physiol. Plant Mol. Biol. 45 (1994) 421-445.

[20] A. Löffler, S. Abel, W. Jost, J.J. Beintema, K. Glund, Phosphate-regulated induction of intracellular ribonuclease in cultured tomato (*Lycopersicon esculentum*) cells, Plant Physiol. 98 (1992) 1472-1478.

[21] T. Nürnberger, S. Abel, W. Jost, K. Glund, Induction of an extracellular ribonuclease in cultured tomato cells upon phosphate starvation, Plant Physiol. 92 (1990) 970-976.

[22] A. Kondracka, A.M. Rychter, The role of Pi recycling processes during photosynthesis in phosphate-deficient bean plants, J. Ext. Bot. 48 (1997) 1461-1468.

[23] L.V. Kochian, Cellular mechanisms of aluminum toxicity and resistance in plants, Ann. Rev. Plant Physiol. Plant Mol. Biol. 46 (1995) 237-260.

[24] L.V. Kochian, O.A. Hoekenga, M.A. Piñeros, How do crop plants tolerate acid soil? Mechanisms of aluminum tolerance and phosphorus efficiency, Ann. Rev. Plant Biol. 55 (2004) 459-493.

[25] R.E. Paull, R.L. Jones, Studies on the secretion of maize root cap slime II. Localization of slime production, Plant Physiol. 56 (1975) 307-312.

[26] S.F. Moody, A.E. Clark, A. Bacic, Structure analysis of secreted slime from wheat ant cowpea roots, Phytochemistry 27, (1988) 2861-2875.

[27] J.F. Ma, S. Hiradate, Form of aluminium for uptake and translocation in buckwheat (*Fagopyrum esculentum* Moench), Planta 211 (2000) 355-360.

[28] J.P. Hammond, M.J. Bennett, H.C. Bowen, M.R. Broadley, D.C. Eastwood, S.T. May, C. Rahn, R. Swarup, K.E. Woolaway, P.J. White, Changes in gene expression in Arabidopsis shoots during phosphate starvation and the potential for developing smart plants, Plant Physiol. 132 (2003) 578-596.

[29] U.P. John, G.C. Spangenberg, Xenogenomics: genomic bioprospecting in indigenous and exotic plants through EST discovery, cDNA microarray-based expression profiling and functional genomics, Comp. Funct. Genom. 6 (2005) 230-235.

[30] C. Uhde-Stone, K.E. Zinn, M. Ramirez-Yáñez, A. Li, C.P. Vance, D.L. Allan, Nylon filter arrays reveal differential gene expression in proteoid roots of white lupin in response to phosphorus deficiency, Plant Physiol. 131 (2003) 1064-1079.

[31] Y.H. Wang, D.F. Gravin, L.V. Kochian, Rapid induction of regulatory and transporter genes in response to phosphorus, potassium, and iron deficiencies in tomato roots. Evidence for cross talk and root/rhizosphere-mediated signals, Plant Physiol. 130 (2002) 1361-1370.

[32] J. Wasaki, R. Yonetani, S. Kuroda, T. Shinano, J. Yazaki, F. Fujii, K. Shimbo, K. Yamamoto, K. Sakata, T. Sasaki, N. Kishimoto, S. Kikuchi, M. Yamagishi, M. Osaki, Transcriptomic analysis of metabolic changes by phosphorus stress in rice plant roots, Plant Cell Envir. 26 (2003) 1515-1523.

[33] P. Wu, L. Ma, X. Hou, M. Wang, Y. Wu, F. Liu, X.W. Deng, Phosphate starvation triggers distinct alterations of genome expression in Arabidopsis roots and leaves, Plant Physiol. 132 (2003) 1260-1271.

[34] K. Xiao, G.H. Bai, B. F. Carver, Nylon filter arrays reveal differential expression of expressed sequence tags in wheat roots under aluminum stress. J Integr. Plant Bio. 47 (2005) 839-848.

[35] L. Anderson, J. Seilhamer, A comparison of selected mRNA and protein abundances in human liver, Electrophoresis 18 (1997) 533-537.

[36] H. Konishi, H. Kitano, S. Komatsu, Identification of rice root proteins regulated by gibberellin using proteome analysis, Plant Cell Envir. 28 (2005) 328-339.

[37] A. Koller, M.P. Washburn, B.M. Lange, N.L. Andon, C. Deciu, P.A. Haynes, L. Hays, D. Schieltz, R. Ulaszek, J. Wei, D. Wolters, J.R. 3rd Yates, Proteomic survey of metabolic pathways in rice, Proc. Natl. Acad. Sci. 99 (2002) 11969-11974.

[38] B. Zhong, H. Karibe, S. Komatsu, H. Ichimura, Y. Nagamura, T. Sasaki, H. Hirano, Screening of rice genes from a cDNA catalog based on the sequence data-file of proteins separated by two-dimensional electrophoresis, Breeding Sci. 47 (1997) 245-251.

[39] M.M. Bradford, A rapid and sensitive method for the quantitation of microgram quantities of protein utilizing the principle of protein–dye binding, Analytical Biochem. 72 (1976) 248–254.

[40] U.K. Laemmli, Cleavage of structural protein during the assembly of head of bacteriophage T4, Nature 227 (1970) 680-685.

[41] R. Ihaka, R.R. Gentleman, Language for data analysis and graphics. J. Graph. Comput. Stat. 5 (1996) 299-314.

[42] Y.H. Yang, S. Dudoit, P. Luu, D.M. Lin, V. Peng, J. Ngai, T.P. Speed, Normalization for cDNA microarray data: a robust composite method addressing single and multiple slide systematic variation. Nucl. Acids Res. 30 (2002) e15.

[43] P. Edman, Method for determination of the amino acid sequence in peptides, Acta Chemica Scandinavica 4 (1950) 277-293.

[44] T. Toda, N. Kimura, Standardization of protocol for Immobiline 2-D PAGE and construction of 2-D PAGE protein database on World Wide Web home page, Jpn. J. Electrophoresis 41 (1997) 13-20.

[45] D.N. Perkins, D.J. Pappin, D.M. Creasy, J.S. Cottrell, Probability-based protein identification by searching sequence databases using mass spectrometry data, Electrophoresis 20 (1999) 3551-3567.

[46] B. Meriga, B.K. Reddy, K.R. Rao, L.A. Reddy, P.B.K. Kishor, Aluminium-induced production of oxygen radicals, lipid peroxidation and DNA damage in seedlings of rice (*Oryza sativa*), J. Plant Physiol. 161 (2004) 63-68.

[47] S.U. Wallace, I.C. Anderson, Aluminium toxicity and DNA synthesis in wheat roots, Agron. J. 76 (1984) 5-8.

[48] Y. Yamaguchi, Y. Yamamoto, H. Matsumoto, Cell death process initiated by a combination and iron in suspension cultures of tobacco cells (*Nicotiana tabacum*). Apotosis-like cell death mediated by calcium and proteinase, Soil Sci. Plant Nutr. 45 (1999) 647-657.

[49] H. Matsumoto, Biochemical mechanism of the toxicity of aluminium and the sequestration of aluminium in plant cells, in: R.J. Wright, V.C. Baligar, R.P. Murrmann, (Eds.), Plant-Soil Interactions at Low-pH. Kluwer, Dordrecht, the Netherlands, 1991, pp. 825-838.

[50] G.J.D. Kirk, E.E. Santos, G.R. Findenegg, Phosphate solubilization by organic anion excretion from rice (*Oryza sativa* L.) growing in aerobic soil, Plant Soil 211 (1999) 11-18.

[51] H.H. Begum, M. Osaki, T. Shinano, H. Miyatake, J. Wasaki, T. Yamamura, T. Watanabe, The function of a maize-derived phosphoenolpyruvate carboxylase (PEPC) in phosphorus-deficient transgenic rice, Soil Sci. Plant Nutr. 51 (2005) 497-506.

[52] M. Nanamori, T. Shinano, J. Wasaki, T. Yamamura, I.M. Rao, M. Osaki, Low phosphorus tolerance mechanisms: phosphorus recycling and photosynthate partitioning in the tropical forage grass, *Brachiaria* Hybrid cultivar Mulato compared with rice, Plant Cell Physiol. 45 (2004) 460-469.

[53] N. Massot, B. Nicander, J. Barceló, Ch. Poschenrieder, E. Tillberg, A rapid increase in cytokinin levels and enhanced ethylene evolution precede Al^{3+}-induced inhibition of root growth in bean seedlings (*Phaseolus vulgaris* L.), Plant Growth Regul. 37 (2002) 105-112.

[54] B.A. Moffatt, Y.Y. Stevens, M.S. Allen, J.D. Snider, L.A. Pereira, M.I. Todorova, P.S. Summers, E.A. Weretilnyk, L. Martin-McCaffrey, C. Wagner, Adenosine kinase deficiency is associated with developmental abnormalities and reduced transmethylation, Plant Physiol. 128 (2002) 812-821.

[55] W.J. Horst, A. Wagner, H. Marschner, Mucilage protects root meristems from aluminum injury, Z. Pflanzenphysiol. 105 (1982) 435-444.

[56] M. Mensch, J.L. Morel, A. Guckert, Metal binding properties of high molecular weight soluble exudates from maize (*Zea mays* L.) roots, Biol. Fertil. Soils 3 (1987) 165-169.

[57] B. Shen, C. Li, M.C. Tarczynski, High free-methionine and decreased lignin content result from a mutation in the *Arabidopsis S*-adenosyl-L-methionine synthetase 3 gene, Plant J. 29 (2002) 371-380.

Figure Legends

Figure 1 Master image, produced as a composite of all analyzed gel images. Image was scanned and analyzed as described in Materials and Methods. The horizontal axis is the isoelectric focusing for first dimension from pI 3 (left) to pI 10 (right). The vertical axis is SDS-PAGE for second dimension from about 27 kDa (bottom) to at least 99 kDa (top). The protein spot number was indicated under every 94 spots (all cross symbol), which were selected at random for peptide mass fingerprinting analysis, resulted in the identification of 56 spots (red cross symbol).

Figure 2 Carbon metabolism map with proteomic alterations. Alterations of identified protein expression were shown with ssp No. The alteration at each time point for both treatments was indicated as colored squares; white, no change; blue and light blue, up-regulated over 2.0 fold and 1.5-2.0 fold, respectively; red and pink, down-regulated over 2.0 fold and 1.5-2.0 fold, respectively. Top and bottom lines indicate the alteration by –P and Al treatment, respectively. DHAP, Dihydroxyacetone phosphate; Fru, Fructose; Fru-1,6-BP, Fructose-1,6-bisphosphate; Glc, Glucose; G-3-P, Glyceraldehyde-3-phosphate;

PGA, phosphoglycerate; 1,3-DPGA, 1,3-Diphosphoglycerate; TP, Triose phosphate.

Supplemental Figure 1 Hierarchical cluster analysis of the entire 464 protein spots. As the results, 10 clusters could be grouped as homogeneous. Left graphs (a) indicate the modifications of root protein expression under both P deficiency and Al stress. Right Venn diagrams (b) show the number of co-expression spots in each cluster.

Table 1 Rice root growth under low P, Al stress under low pH conditions

g FW/plant	0 d	0.5 d	1 d	3 d	5 d	10 d
control	1.74±0.05	1.64±0.14	1.61±0.08	1.67±0.12	2.01±0.14	2.19±0.08
-P		1.62±0.09	1.72±0.13	1.91±0.10	2.10±0.11	2.38±0.11
+Al		1.44±0.08	1.63±0.08	1.52±0.10	1.72±0.04*	

mean ±SE, n = 4, *n = 8

Table 2 Rice root proteins expressed under low P, Al stress under low pH conditions

SSP	Accession No.	Identified protein	Mass (kDa)	Calculated pI	Alteration of Expression [log_2(-P/+P)] 0.5 d	1 d	3 d	5 d	10 d	Alteration of Expression [log_2(+Al/-Al) 0.5 d	1 d	3 d	5 d
(i) C metabolism													
4911	BAD05751	Putative Aconitate hydratase	98.6	5.67	0.27	2.18	-0.47	-1.32	2.05	-0.71	1.81	0.64	0.22
4801	BAB19388	Putative transketolase	80.5	6.12	0.10	0.72	-0.55	-0.23	-0.35	-0.19	0.71	-0.20	0.30
4804	BAB19388	Putative transketolase	80.5	6.12	-0.14	0.85	-0.27	-0.49	0.00	-0.11	0.77	-0.60	-0.04
5708	BAC83515	Putative succinate dehydrogenase flavoprotein alpha subunit	69.5	6.61	-0.24	0.13	0.17	-0.04	0.03	0.04	0.17	0.22	-2.78
4711	NP_916713	P0022F10.12 protein (Malic enzyme)	65.8	5.79	-0.04	0.29	0.62	-0.59	1.10	0.22	0.21	-1.10	-0.01
4701	BAB62580	Putative 2,3-bisphosphoglycerate-independent phosphoglycerate mutase	61.2	5.53	0.26	0.06	0.25	-0.41	-0.34	-0.08	-0.13	0.75	0.34
4608	AAK16194	Putative UDP-glucose dehydrogenase	53.4	5.79	0.29	0.34	-0.76	-0.15	1.18	0.34	-0.56	-0.89	-0.01
5511	NP_910282	Cytosolic 6-phosphogluconate dehydrogenase	53.0	5.85	-0.08	0.51	0.14	0.22	0.70	0.10	-0.37	-0.12	0.07
6603	NP_908725	Putative dihydrolipoamide dehydrogenase	53.0	7.21	0.36	-0.09	0.80	0.15	-0.05	0.81	-1.26	0.15	0.72
6501	AAG28777	Citrate synthase	52.4	7.71	-0.25	-0.30	-0.23	0.11	0.10	-0.12	-0.45	-0.46	-0.25
4503	BAB69069	UDP-glucose pyrophosphorylase	51.8	5.43	-0.13	-0.69*	2.57	-0.13	0.27	0.13	0.23	2.56	0.18
2505	NP_917673	Putative acetyl transferase	46.9	4.96	0.21	-0.02	-0.08	-0.49	0.32	-0.13	0.40	-0.20	-0.27
5416	NP_917313	NADP-specific isocitrate dehydrogenase	46.4	6.34	-0.05	-0.01	-0.04	0.40	-0.12	0.04	-0.27	-0.11	-0.04
5307	CAD79700	Putative glyceraldehyde 3-phosphate dehydrogenase	42.4	6.41	-0.69	0.62	-1.54**	-1.74	0.50	-0.80	-1.07	-1.82*	-1.70
5310	CAD79700	Putative glyceraldehyde 3-phosphate dehydrogenase	42.4	6.41	-0.09	-0.02	-0.11	-0.09	0.85	-0.29	-0.41	-0.27	-0.32
6304	CAD79700	Putative glyceraldehyde 3-phosphate dehydrogenase	42.4	6.41	-0.09	-0.31	0.28	-0.76	-0.30	0.16	-1.21	-0.01	-0.87
5410	AAF34412	Alcohol dehydrogenase 2	42.0	6.04	0.27	0.44	0.46	0.98	0.84	-0.35	0.62	0.68	0.72
6410	P17784	Fructose-bisphosphate aldolase, cytoplasmic isozyme	39.2	8.50	-0.43	-0.66	-0.41	0.14	-0.16	-0.38	-0.25	-0.24	-1.01
3314	NP_919911	Putative aldose 1-epimerase - like protein	37.3	5.44	0.00	-2.13	-2.15	0.00	0.00	3.56	-1.97	-2.11	0.00
2312	AAL26573	Putative fructokinase Ⅱ	35.9	5.02	0.21	0.24	0.04	0.16	-0.09	0.06	0.21	-0.03	0.24
4311	NP_921996	Cytoplasmic malate dehydrogenase	35.9	5.75	0.10	0.03	0.04	0.21	-0.01	-0.09	0.11	0.00	0.37
5306	NP_917241	Putative malate dehydrogenase	35.7	8.74	-0.02	-1.46*	-0.44	-0.06	0.09	0.04	-0.46	0.11	-0.33
2311	NP_915138	Putative fructokinase Ⅰ	34.9	5.07	0.72	-0.33	0.31	-0.30	0.65	1.18*	-0.20	0.30	-0.27
3307	BAB71741	Glyoxalase Ⅰ	32.9	5.51	-0.08	-0.31	-0.03	0.37	0.10	0.14	-0.02	0.19	0.52
3106	NP_909244	Putative triose-phosphate isomerase	27.3	5.38	0.28	0.06	0.36	0.58	-0.76	0.22	0.08	0.22	0.53
7301	AAN59792	Cytosolic glyceraldehyde-3-phosphate dehydrogenase GAPDH	23.5	7.88	-0.03	-0.60	-0.12	0.67	3.31	-0.81	-0.85	1.12**	0.61
7305	AAN59792	Cytosolic glyceraldehyde-3-phosphate dehydrogenase GAPDH	23.5	7.88	-0.28	-1.16	-0.49	0.21	3.61	0.31	0.16	0.10	-0.43
(ii) N metabolism													
5414	AAO37984	Glutamate dehydrogenase	44.6	6.15	0.11	-0.06	-0.07	0.04	0.23	0.03	0.00	-0.30	-3.04
2412	AAP50991	Putative 3-isopropylmalate dehydrogenase	43.5	5.85	1.20	0.31	0.35	0.10	-0.43	0.99*	0.66	0.56	0.24
3413	P14656	Glutamine synthetase shoot isozyme	39.4	5.51	0.12	-0.01	-0.24	-0.06	-0.50*	-0.03	-0.51	-0.14	0.54
4407	NP_912586	Putative gln1_oryza glutamine synthtase root isozyme(glutamate--ammonia	38.8	5.73	0.20	0.30	0.06	-0.12	-1.01**	0.00	0.34	0.36*	0.38
(iii) Nucleotide Related													
2807	S53126	DnaK-typez molecular chaperone hsp70 (fragment)	71.5	5.13	0.38	0.62	-0.48	-1.09	-0.44	0.19	-0.28	-0.81	0.00
3603	Q01859	ATP synthase β chain, mitochondrial precursor	59.1	6.30	0.30	0.08	-0.49	-0.44	0.15	0.46	-0.26	0.07	0.38
2604	AAK54617	Vacuolar ATPase B subunit	54.1	5.07	0.08	0.01	0.14	0.49	0.38	0.25	0.34	0.24	0.57
5303	NP_916988	Guanine nucleotide-binding protein β subject-like protein (GPB-LR) (RWD	36.7	5.97	-0.01	-1.69	0.99	0.24	-0.22	-0.02	0.38	0.79*	-0.12
2410	AAO72629	Adenosin kinase	32.6	5.29	0.16	-0.10	2.12	-0.02	-2.86	-0.01	-0.09	2.18	0.04
3311	NP_916608	Putative cytidine deaminase	32.2	5.13	1.08	1.64	0.64	2.23*	2.00	0.34	1.65	0.37	1.77
2303	Q40680	Elongation factor 1-β (EF-1-BETA)	24.9	4.36	-0.68	-1.77	0.71	3.55	0.64	0.25	-0.76	-1.00	2.30
2509	BAB78504	26S proteasome regulatory particle triple-A ATPase subunit5b	21.9	5.51	1.14	-2.05	3.42	-2.14	0.00	0.18	-1.14	1.66	-3.38
(iv) Oxidation/Reduction													
2701	AAP50932	Putative trypanothione-dependent peroxidase	65.2	4.82	0.70	-0.90	0.24	1.37	-0.73	0.44	0.30	1.31	2.53*
2711	AAP50932	Putative trypanothione-dependent peroxidase	64.4	4.82	0.52	0.77	0.29	-0.08	0.38	0.61	0.63	-0.20	0.01
3409	BAD09086	Monodehydroascorbate reductase (fragment)	46.8	5.30	-0.04	-0.12	-0.43	-0.31	-0.60*	0.05	0.30	0.15	0.21
5309	BAD07786	Putative NADPH-thioredoxin reductase	34.9	6.19	-1.37	-0.71	0.22	0.31	1.57	-0.56	-0.25	-0.07	0.26
3105	T03595	L-ascorbate peroxidase	27.3	5.42	-0.36	-0.15	0.32	-0.24	-0.08	-0.23	-0.03	0.10	-1.18
4101	T03595	L-ascorbate peroxidase	27.3	5.42	-0.15	0.06	0.29	0.28	-0.07	0.02	0.04	-0.07	0.22
3202	BAB17666	Ascorbate peroxidase	27.2	5.21	-0.03	-0.14	-0.05	-0.24	-0.36*	-0.10	-0.20	-0.07	0.09
5102	NP_916246	Glutathione S-tranferase Ⅱ	24.3	5.77	-0.08	0.42	0.81	0.66*	0.30	0.11	0.08	0.42	-0.06
(v) Others													
3903	NP_921687	Putative endoplasmic reticulum membrane fusion protein	91.6	5.07	2.41	3.47	0.32	0.00	-1.35	1.23	3.65	-0.60	-0.22
3414	AAO41148	Putative IAA amidohydrolase	44.1	5.44	2.23	-0.65	-3.96	-0.29	2.44	2.26*	-2.29	0.76	-3.54
5402	CAC82203	S-adenosylmethionine synthetase	43.6	5.93	-0.15	0.30	0.04	-0.36	-0.08	0.53*	0.92**	1.26*	0.87
4416	P93438	S-adenosylmethionine synthetase 2 (Methionine adenosyl transferase 2)	43.3	5.68	-0.11	0.10	0.24	-0.17	0.18	0.77**	0.06	1.07*	0.99
3407	ATRZ1	Actin 1 - rice	42.1	5.22	-0.05	-0.87	0.87	0.18	0.73	0.50**	0.75	0.61	0.23
4417	CAA77235	Reversibly glycosylated polypeptide	41.8	5.82	0.04	-0.25	-0.11	0.00	-0.08	0.03	-0.15	-0.52	-0.32
3402	NP_915638	Putative actin	40.0	5.39	0.14	-0.73	0.99	-0.51	0.69	0.63**	0.72	0.91	-0.08
3411	BAC99512	Putative Caffeic acid 3-O-methyltransferase	39.7	5.41	-0.07	0.44	-0.03	0.33	0.33	-0.20	0.31	-0.25	0.02
2713	BAA92322	Protein disulfide isomerase (fragment)	33.5	4.81	0.06	0.04	0.32	0.32	-0.50	0.23	-0.11	0.14	0.06

* significant difference was found by ANOVA (p <0.05)
** significant difference was found by ANOVA (p <0.01)

up-regulated (over 2 fold)
up-regulated (1.5-2.0 fold)
down-regulated (over 2 fold)
down-regulated (1.5-2.0 fold

pI

4.0

6.0

8.0

kDa

—99

—27

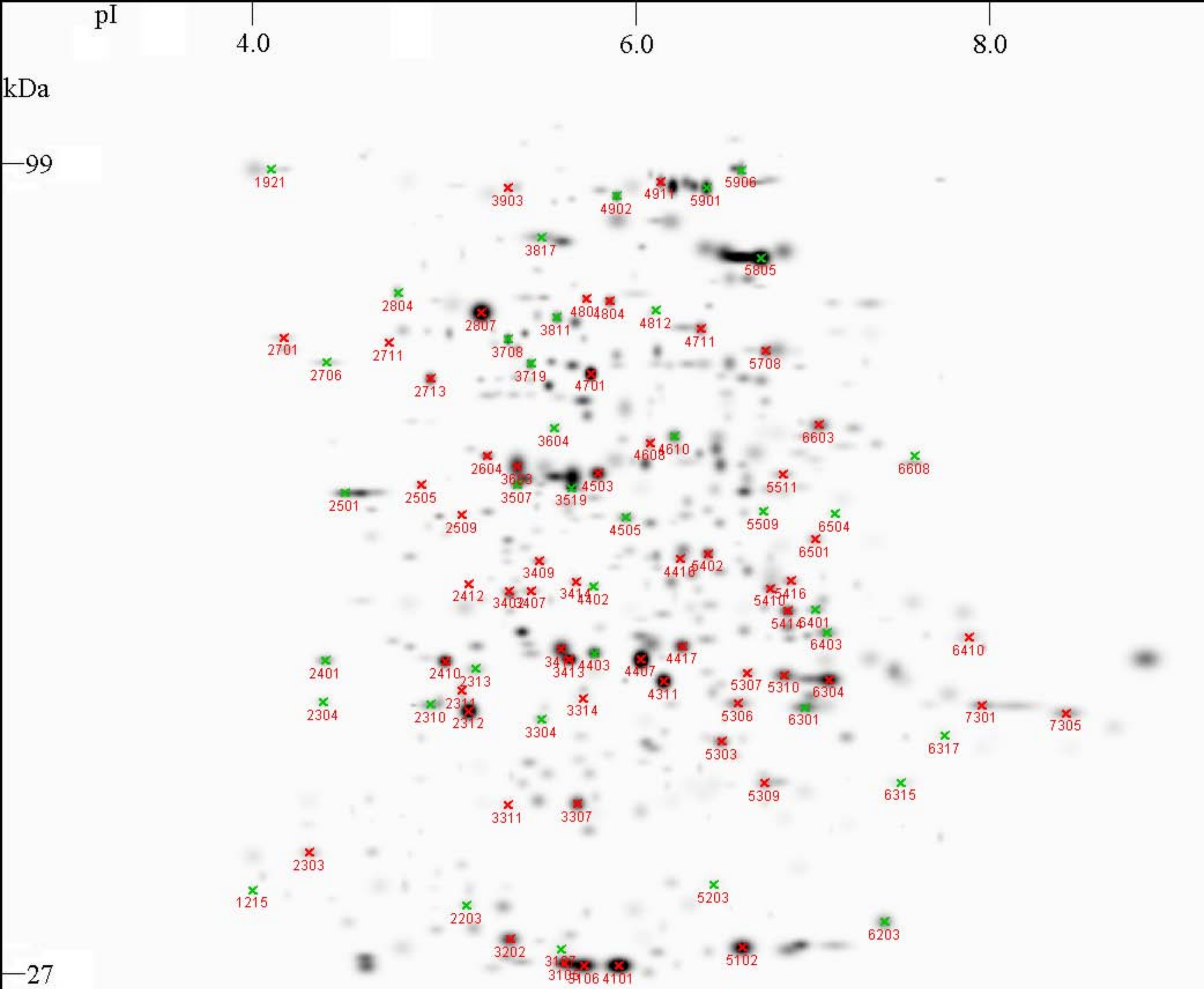

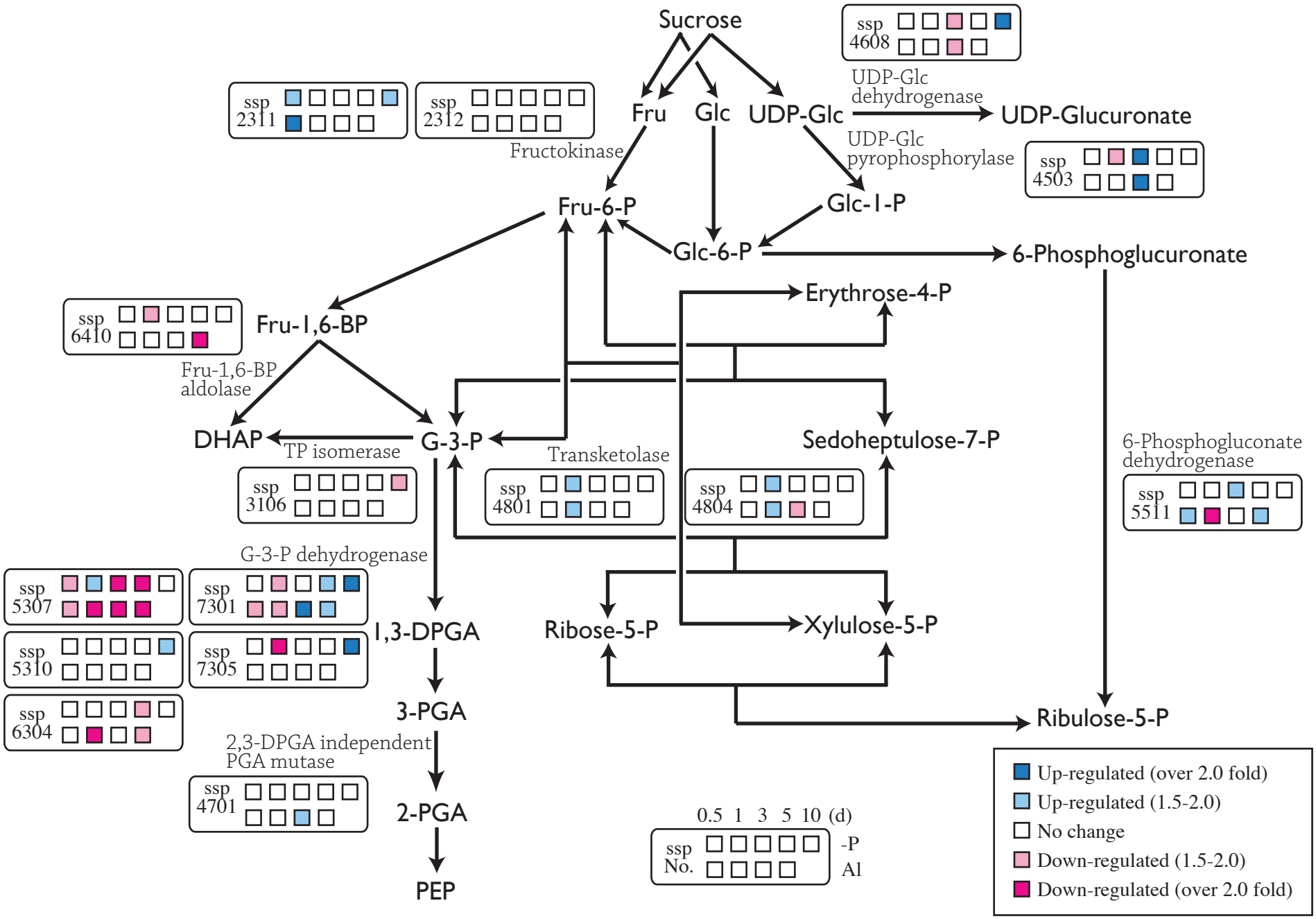
Sucrose
Fru
Glc
UDP-Glc
UDP-Glucuronate
UDP-Glc dehydrogenase
UDP-Glc pyrophosphorylase
Fructokinase
Fru-6-P
Glc-1-P
Glc-6-P
6-Phosphoglucuronate
Erythrose-4-P
Fru-1,6-BP
Fru-1,6-BP aldolase
DHAP
TP isomerase
G-3-P
Transketolase
Sedoheptulose-7-P
6-Phosphogluconate dehydrogenase
G-3-P dehydrogenase
1,3-DPGA
Ribose-5-P
Xylulose-5-P
3-PGA
Ribulose-5-P
2,3-DPGA independent PGA mutase
2-PGA
PEP
ssp 4608
ssp 2311
ssp 2312
ssp 4503
ssp 6410
ssp 3106
ssp 4801
ssp 4804
ssp 5511
ssp 5307
ssp 7301
ssp 5310
ssp 7305
ssp 6304
ssp 4701
0.5 1 3 5 10 (d)
ssp No.
-P
Al
Up-regulated (over 2.0 fold)
Up-regulated (1.5-2.0)
No change
Down-regulated (1.5-2.0)
Down-regulated (over 2.0 fold)

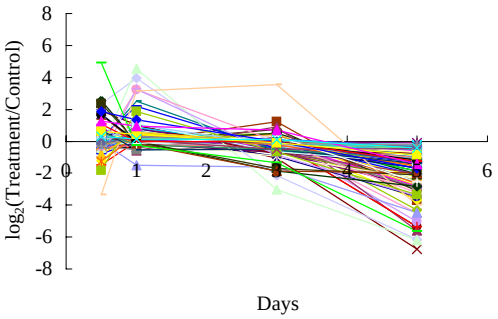

Cluster 1 (a)

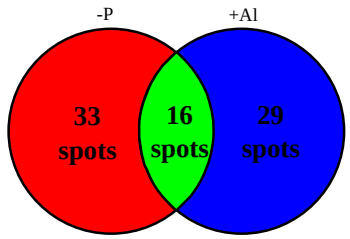

Cluster 1 (b)

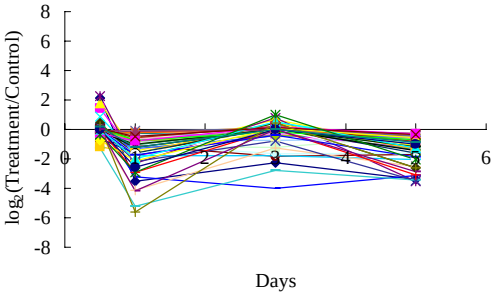

Cluster 2 (a)

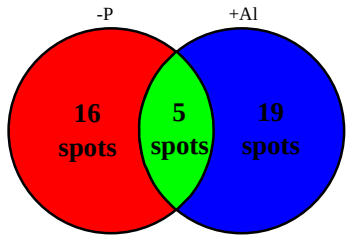

Cluster 2 (b)

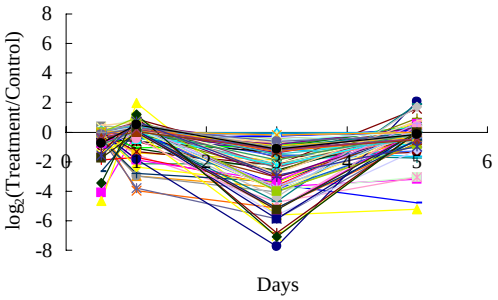

Cluster 3 (a)

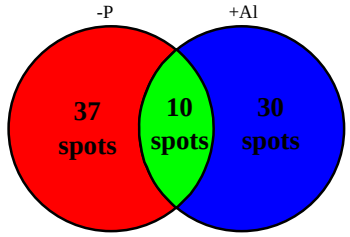

Cluster 3 (b)

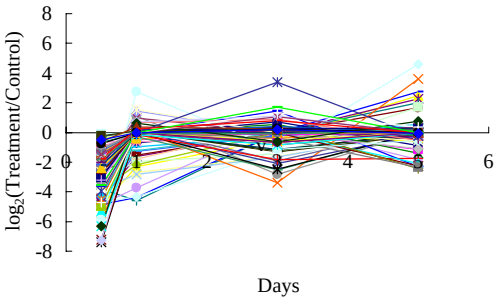

Cluster 4 (a)

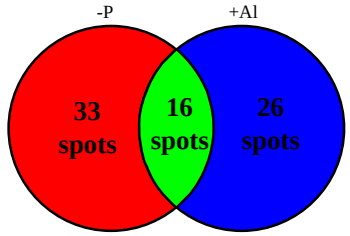

Cluster 4 (b)

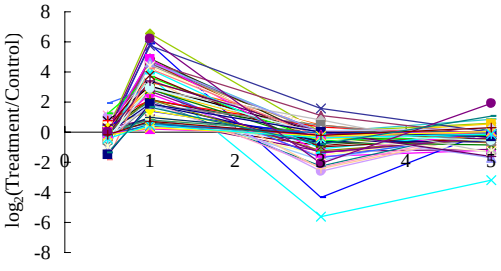

Cluster 5 (a)

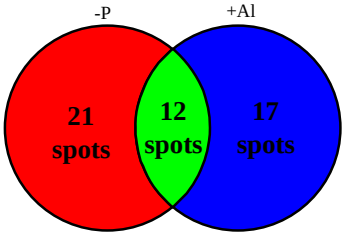

Cluster 5 (b)

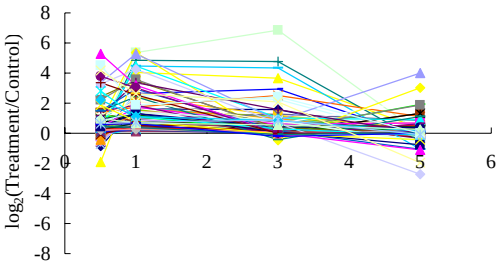

Cluster 6 (a)

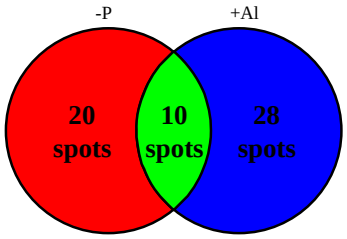

Cluster 6 (b)

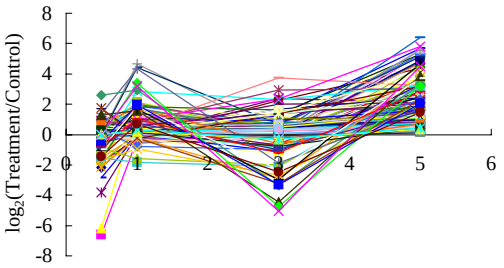

Cluster 7 (a)

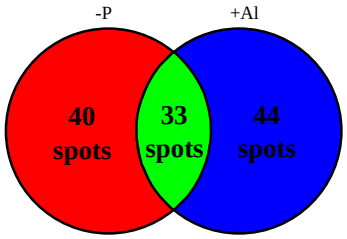

Cluster 7 (b)

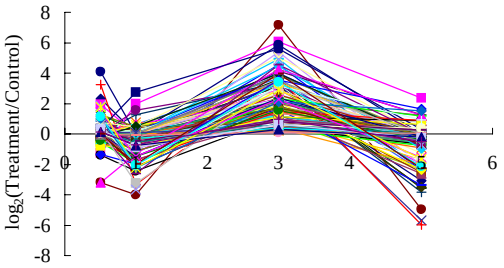

Cluster 8 (a)

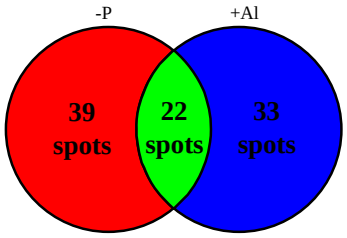

Cluster 8 (b)

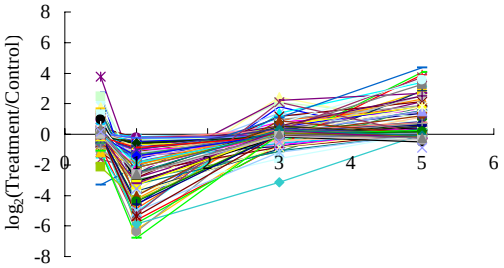

Cluster 9 (a)

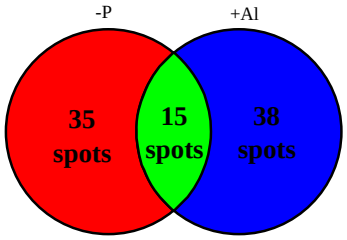

Cluster 9 (b)

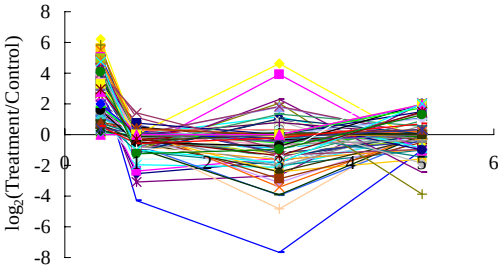

Cluster 10 (a)

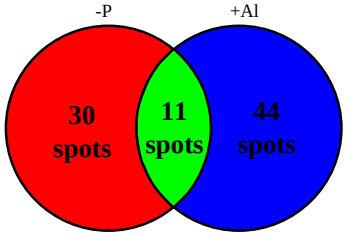

Cluster 10 (b)